Hindawi
International Journal of Antennas and Propagation
Volume 2019, Article ID 3849791, 9 pages
https://doi.org/10.1155/2019/3849791

Research Article

A Sparse Representation Method for Coherent Sources Angle Estimation with Uniform Circular Array

Xiaolong Su, Zhen Liu, Tianpeng Liu, Bo Peng, Xin Chen, and Xiang Li

College of Electronic Science and Technology, National University of Defense Technology, Changsha 410073, China

Correspondence should be addressed to Zhen Liu; zhen_liu@nudt.edu.cn

Received 19 June 2019; Revised 9 September 2019; Accepted 19 September 2019; Published 10 October 2019

Academic Editor: Ahmed Toaha Mobashsher

Coherent source localization is a common problem in signal processing. In this paper, a sparse representation method is considered to deal with two-dimensional (2D) direction of arrival (DOA) estimation for coherent sources with a uniform circular array (UCA). Considering that objective function requires sparsity in the spatial dimension but does not require sparsity in time, singular value decomposition (SVD) is employed to reduce computational complexity and ℓ_2 norm is utilized to renew objective function. After the new objective function is constructed to evaluate residual and sparsity, a second-order cone (SOC) programming is employed to solve convex optimization problem and obtain 2D spatial spectrum. Simulations show that the proposed method can deal with the case of coherent source localization, which has higher resolution than 2D MUSIC method and does not need to estimate the number of coherent sources in advance.

1. Introduction

Direction of arrival (DOA) parameter estimation using sensor arrays has been an active research area and plays a fundamental role in many applications involving radar, sonar, electronic warfare, seismic exploration, etc. [1, 2]. By employing uniform linear array (ULA), many advanced techniques have been proposed to achieve superresolution localization [3]. However, the configuration of ULA can only provide one-dimensional (1D) DOA estimation within 180 degrees [4].Besides, the resolution of the ULA in the normal direction is satisfactory, which results in an effective estimation only for one-dimensional (1-D) DOA within 120 degrees [5]. In contrast, uniform circular array (UCA) can provide 360° azimuthal coverage and additional elevation angle information [6], which is an attractive geometry in the context of two-dimensional (2D) DOA parameter estimation [7].

Some superresolution algorithms are able to obtain DOA estimation under the assumption that the sources are incoherent [8, 9]. However, coherent source localization is a common problem in the signal processing [10]. The presence of coherent sources will lead to performance degradation and even invalidation of parameter estimation. The coherent sources appear in specular multipath propagation or in military scenarios involving cochannel interference [11]. Unfortunately, due to the fact that the rank of covariance matrix is less than the number of coherent sources, the traditional beamspace domain methods such as MUSIC or ESPRIT cannot achieve source localization effectively [12]. Therefore, research on the localization algorithm of coherent sources is a significant part of array signal processing. Based on the l_1 norm constraint and singular value decomposition (SVD), Malioutov et al. [13] employed ULA and extended the idea of enforcing sparse representation (SR) to estimate the elevation angle of coherent sources. Yet, it can only achieve 1D DOA estimation.

Although the UCA-MUSIC algorithm and UCA-ESPRIT algorithm in the study by Mathews and Zoltowski [14] have employed uniform circular array to achieve the azimuth angle and elevation angle estimation of multiple sources in space, it is required that the sources are

incoherent and will be invalid when the sources have the same frequencies.

Accordingly, we present a sparse representation algorithm that extends the method in previous studies [15–17] for 2D DOA parameter estimation of coherent sources under an UCA. Herein, after the received signal is transformed into a sparse representation framework, we utilize singular value decomposition (SVD) of the data matrix to reduce computational complexity and compute the ℓ_2 norm of time samples in spatial index. Due to the fact that the second-order cone (SOC) programming is an efficient interior point algorithm, which is suitable for optimizing functions that contain convex quadratic and linear terms [18], we apply SOC scheme to solve convex optimization problem and obtain superresolution spatial spectrum. Simulation experiments are carried out to verify that the proposed approach does not need to estimate the number of coherent sources in advance and has higher resolution than 2D MUSIC method for coherent source localization.

2. Signal Modeling

Consider an UCA in the xy plane with radius R and M identical omnidirectional sensors impinged by Q coherent narrowband sources. The coherent narrowband sources have the same frequency and wavelength. The sensors are uniformly and counterclockwise spaced on the circumference where the first sensor is located at the x-axis, its geometry is shown in Figure 1. The 2D DOA of qth source is described as (ϕ_q, θ_q), where the azimuth angle $\phi_q \in [-\pi, \pi)$ is measured counterclockwise from the x-axis, and the elevation angle $\theta_q \in [0, \pi/2]$ is measured downward from the z-axis. The output of the mth sensor of the UCA at the nth sample is given by

$$x_m(n) = \sum_{q=1}^{Q} s_q\left(n - \tau_{m,q}\right) + w_m(n), \tag{1}$$

for $m = 1, 2, \ldots, M$ and $n = 1, 2, \ldots, N$, $s_q(n)$ represents the qth narrowband time sampling with power $\sigma_{s,q}^2$, and $w_m(n)$ is assumed to be a zero-mean white complex Gaussian noise at the mth sensor. When taking array center as a benchmark, $\tau_{m,q}$ is the propagation delay of the mth sensor for the qth narrowband source and can be expressed as

$$\tau_{m,q} = \frac{R\zeta_m\left(\phi_q, \theta_q\right)}{c}, \tag{2}$$

where c is the speed of light, $\zeta_m(\phi_q, \theta_q) = \cos(\gamma_m - \phi_q)\sin\theta_q$ with $\gamma_m = (2\pi(m-1))/M$.

Substituting (2) into (1) yields the signal model

$$x_m(n) = \sum_{q=1}^{Q} s_q(n) e^{j\left(2\pi R/\lambda_q\right)\zeta_m\left(\phi_q, \theta_q\right)} + w_m(n), \tag{3}$$

where λ_q represents the wavelength of the qth narrowband source, and the coherent sources have the same wavelength.

In matrix form, the output of UCA can be written as

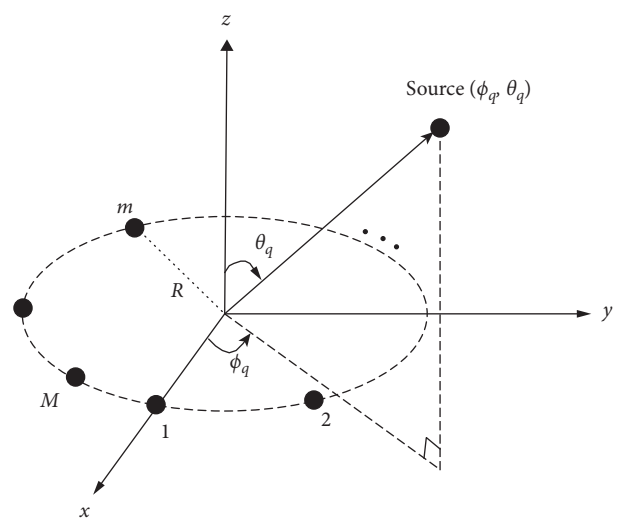

Figure 1: Geometry of an UCA with a narrowband source.

$$\mathbf{X} = \mathbf{AS} + \mathbf{W}, \tag{4}$$

$$\mathbf{A} = \left[\, \mathbf{a}_1 \;\; \mathbf{a}_2 \;\; \ldots \;\; \mathbf{a}_Q \,\right], \tag{5}$$

$$\mathbf{S} = \left[\, \mathbf{s}_1 \;\; \mathbf{s}_2 \;\; \ldots \;\; \mathbf{s}_Q \,\right]^{\mathrm{T}}, \tag{6}$$

$$\mathbf{W} = \left[\, \mathbf{w}_1 \;\; \mathbf{w}_2 \;\; \ldots \;\; \mathbf{w}_M \,\right]^{\mathrm{T}}, \tag{7}$$

with

$$\begin{aligned} a_q &= \left[\, e^{j\left(2\pi R/\lambda_q\right)\zeta_1\left(\phi_q,\theta_q\right)} \;\; e^{j\left(2\pi R/\lambda_q\right)\zeta_2\left(\phi_q,\theta_q\right)} \;\; \ldots \;\; e^{j\left(2\pi R/\lambda_q\right)\zeta_M\left(\phi_q,\theta_q\right)} \,\right]^{\mathrm{T}}, \\ \mathbf{s}_q &= \left[\, s_q(1) \;\; s_q(2) \;\; \ldots \;\; s_q(N) \,\right], \\ \mathbf{w}_m &= \left[\, w_m(1) \;\; w_m(2) \;\; \ldots \;\; w_m(N) \,\right], \end{aligned} \tag{8}$$

where $(\bullet)^{\mathrm{T}}$ denotes the transpose operator.

3. Proposed Algorithm

To obtain the superresolution spatial spectrum of coherent sources, this paper employs sparse representation framework. Especially, considering that the second-order cone (SOC) programming is suitable to solve the convex optimization problem, we employ SOC scheme to obtain 2D DOA spatial spectrum of coherent sources.

3.1. Sparse Representation of Signal Model. The overcomplete representation of source parameter estimation problem with multiple snapshots can be written as

$$\mathbf{X} \approx \widetilde{\mathbf{X}} = \mathbf{BY} + \mathbf{W}, \tag{9}$$

where

$$\mathbf{B} = \left[\, \mathbf{b}_1 \;\; \mathbf{b}_2 \;\; \ldots \;\; \mathbf{b}_K \,\right], \tag{10}$$

$$\mathbf{Y} = \left[\, \mathbf{y}_1 \;\; \mathbf{y}_2 \;\; \ldots \;\; \mathbf{y}_K \,\right]^{\mathrm{T}}, \tag{11}$$

$$\mathbf{W} = [\,\mathbf{w}_1 \;\; \mathbf{w}_2 \;\; \ldots \;\; \mathbf{w}_M\,]^{\mathrm{T}}, \tag{12}$$

with

$$\begin{aligned}
\mathbf{b}_k &= \left[\, e^{j(2\pi R/\lambda_k)\zeta_1(\widetilde{\phi}_k,\widetilde{\theta}_k)} \;\; e^{j(2\pi R/\lambda_k)\zeta_2(\widetilde{\phi}_k,\widetilde{\theta}_k)} \;\; \ldots \;\; e^{j(2\pi R/\lambda_k)\zeta_M(\widetilde{\phi}_k,\widetilde{\theta}_k)} \,\right]^{\mathrm{T}},\\
\mathbf{y}_k &= [\, y_k(1) \;\; y_k(2) \;\; \ldots \;\; y_k(N)\,],\\
\mathbf{w}_m &= [\, w_m(1) \;\; w_m(2) \;\; \ldots \;\; w_m(N)\,],
\end{aligned} \tag{13}$$

for $k = 1, 2, \ldots, K$, $\mathbf{B} \in \mathbb{C}^{M\times K}$ is referred to as a dictionary with $Q \ll K$, $(\widetilde{\phi}, \widetilde{\theta})$ represents the combination of azimuth angle and elevation angle that may occur in space. $\mathbf{Y} \in \mathbb{C}^{K\times N}$ is referred to as a sparse representation of the received data $\mathbf{X} \in \mathbb{C}^{M\times N}$ with respect to the dictionary.

Considering that sparsity only has to be enforced in space, the ℓ_2 norm of time samples in spatial index is computed and defined as

$$\widetilde{y}_k = \|\mathbf{Y}_k\|_2 = \sqrt{\sum_{n=1}^{N} (\mathbf{Y}_k(n))^2}, \tag{14}$$

for $k = 1, 2, \ldots, K$, $\|\bullet\|_2$ represents ℓ_2 norm, $\mathbf{Y}_k(n)$ represents the kth row and the nth column element in matrix $\mathbf{Y}$. If $(\widetilde{\phi}_k, \widetilde{\theta}_k)$ in (10) and (ϕ_q, θ_q) in (5) are equal or close, the complex amplitude in the kth element of vector $\widetilde{y} = [\widetilde{y}_1, \widetilde{y}_2, \ldots, \widetilde{y}_K]$ is not zero and corresponds to the DOA of sources. Therefore, the DOA estimation problem is translated into estimating the position of nonzero element in vector $\widetilde{y}$. The objective function of sparse representation method that extends the method in [13] can be written as

$$\min\left(\|\mathbf{X} - \mathbf{BY}\|_{\mathrm{F}} + \mu\|\widetilde{y}\|_1\right), \tag{15}$$

where $\|\cdot\|_{\mathrm{F}}$ represents Frobenius norm, $\|\cdot\|_1$represents ℓ_1 norm, $\|\mathbf{X} - \mathbf{BY}\|_{\mathrm{F}} = \|\mathrm{vec}(\mathbf{X} - \mathbf{BY})\|_2$ is utilized to evaluate the size of the residual, $\|\widetilde{y}\|_1$ is utilized to evaluate the sparsity of the representation in space dimension, parameter μ in the objective function controls the tradeoff between the residual and sparsity.

3.2. Singular Value Decomposition and Dimension Reduction. Considering that the objective function requires sparsity in the spatial dimension but does not require sparsity in time, the singular value decomposition (SVD) is utilized to reduce computational complexity. The SVD of covariance matrix $\mathbf{X}$ can be written as

$$\mathbf{X} = \mathbf{U\Sigma V}^{\mathrm{H}}, \tag{16}$$

where $(\bullet)^{\mathrm{H}}$ denotes the complex conjugation, $\mathbf{U} \in \mathbb{C}^{M\times M}$ and $\mathbf{V} \in \mathbb{C}^{N\times N}$ are unitary matrices, $\mathbf{\Sigma} \in \mathbb{C}^{M\times N}$ is a positive semidefinite diagonal matrix, and the elements on the diagonal are the singular values of $\mathbf{X}$.

The dimension reduction matrix $\mathbf{X}^{\mathrm{SVD}}$ that contains most of the signal power can be expressed as

$$\mathbf{X}^{\mathrm{SVD}} = \mathbf{XVD}, \tag{17}$$

where $\mathbf{D} = [\mathbf{I}_G, \mathbf{0}]^{\mathrm{H}}$. Here, $\mathbf{I}_G \in \mathbb{C}^{G\times G}$ is an identity matrix, $\mathbf{0} \in \mathbb{C}^{G\times(N-G)}$ is a matrix of zeros, and G is the assumed number of sources that can be more or less than the real number of sources Q. It is noteworthy that the number of coherent sources can be unknown and does not need to be accurately estimated in advance by utilizing the Akaike information criterion (AIC) or the minimum description length (MDL) detection criterion [19].

It can be noticed that the computational complexity is reduced because the size of dimension is changed from matrix $\mathbf{X} \in \mathbb{C}^{M\times N}$ in (4) to matrix $\mathbf{X}^{\mathrm{SVD}} \in \mathbb{C}^{M\times G}$ in (18). Due to the fact that the structural assumptions are not relied on the orthogonality of the signal and noise subspaces, the incorrect number of sources in our framework has no catastrophic consequences and we do not need to estimate the information about the number of sources G in (17) in advance.

In addition, $\mathbf{X}^{\mathrm{SVD}}$ can also be written as

$$\mathbf{X}^{\mathrm{SVD}} = \mathbf{BY}^{\mathrm{SVD}} + \mathbf{W}^{\mathrm{SVD}}, \tag{18}$$

where $\mathbf{Y}^{\mathrm{SVD}} = \mathbf{YVD}$ and $\mathbf{W}^{\mathrm{SVD}} = \mathbf{WVD}$. Considering that sparsity does not to be enforced in time, we combine each line of matrix $\mathbf{Y}^{\mathrm{SVD}}$ by computing

$$\widetilde{y}_k^{\mathrm{SVD}} = \|\mathbf{Y}_k^{\mathrm{SVD}}\|_2 = \sqrt{\sum_{g=1}^{G} \left(\mathbf{Y}_k^{\mathrm{SVD}}(g)\right)^2}, \tag{19}$$

for $k = 1, 2, \ldots, K$, $\|\bullet\|_2$ represents ℓ_2 norm and $\mathbf{Y}_k^{\mathrm{SVD}}(g)$ represents the element of the kth row and the gth column in matrix $\mathbf{Y}^{\mathrm{SVD}}$. Therefore, the peaks of vector $\widetilde{y}^{\mathrm{SVD}} = [\widetilde{y}_1^{\mathrm{SVD}}, \widetilde{y}_2^{\mathrm{SVD}}, \cdots, \widetilde{y}_K^{\mathrm{SVD}}]$ correspond to the DOA of coherent sources. After the dimension is reduced, the unconstrained objective function can be expressed as

$$\min\left(\|\mathbf{X}^{\mathrm{SVD}} - \mathbf{BY}^{\mathrm{SVD}}\|_{\mathrm{F}} + \mu\|\widetilde{y}^{\mathrm{SVD}}\|_1\right). \tag{20}$$

3.3. Second-Order Cone Programming. It can be noticed that (20) is a convex optimization problem. Constraining sparsity with ℓ_2 norm can guarantee to obtain a global optimal solution and can be solved quickly by employing a second-order cone (SOC) scheme. The SOC programming is an efficient interior point algorithm, which is suitable for optimizing functions that contain convex quadratic and linear terms.

The SOC programming form that extends the method in [18] to solve (20) can be expressed as

$$\begin{aligned}
\min \quad & (p_1 + \mu p_2)\\
\text{s.t.} \quad & \left\|\left[(\mathbf{Z}(1))^{\mathrm{T}}, (\mathbf{Z}(2))^{\mathrm{T}}, \ldots, (\mathbf{Z}(G))^{\mathrm{T}}\right]\right\|_2\\
& \le p_1, \|\mathbf{h}\|_1 \le p_2 \text{ and } \|\mathbf{Y}_k^{\mathrm{SVD}}\|_2 \le h_k,
\end{aligned} \tag{21}$$

where $\mathbf{Z} = \mathbf{X}^{\mathrm{SVD}} - \mathbf{BY}^{\mathrm{SVD}}$, $\mathbf{Z}(g)$ represents the gth column of the matrix $\mathbf{Z}$, $\mathbf{Y}_k^{\mathrm{SVD}}$ represents the kth row of the matrix $\mathbf{Y}^{\mathrm{SVD}}$, and h_k represents the kth element of the vector $\mathbf{h}$.

Ultimately, we translate the global optimal solution $\mathbf{Y}^{\mathrm{SVD}}$ into $\widetilde{y}_k^{\mathrm{SVD}}$ according to (19) and search the peaks of spatial spectrum to obtain the 2D DOA of coherent sources.

4. Results and Discussion

In this section, CVX toolbox in Matlab software is utilized to achieve sparse representation programming, and simulation results are performed to demonstrate the effectiveness of our proposed algorithm. The results show that the proposed algorithm does not need to estimate the number of sources in advance and can obtain the accurate 2D DOA estimation of coherent sources.

4.1. Performance of Location. To verify that the proposed algorithm can achieve the localization of coherent sources, an UCA with 16 sensors and fixed radius 5 m are considered in this simulation. Two equal power coherent sources impinge on the UCA from 2D DOA $(\phi = 50^\circ, \theta = 40^\circ)$ and $(\phi = 120^\circ, \theta = 30^\circ)$. The frequencies of the two coherent sources are both set at 100 MHz. The snapshot number N and grid size of angle estimation are set as 50 and 0.1°, respectively. The parameter μ and SNR are set as 2 and 0 dB, respectively. The additive noise is spatial white complex Gaussian random signal. Especially, the assumed number of coherent sources G is set as 2 in this simulation, which can be more or less than the real number of coherent sources.

The 2D spatial spectrum of the mentioned coherent sources is shown in Figure 2, where the red lines represent the real 2D DOA of coherent sources. It can be noticed that the peaks of spatial spectrum are corresponding to 2D DOA of coherent sources. Therefore, we can conclude that the proposed sparse representation algorithm can decouple the coherent sources and achieve the 2D DOA estimation successfully.

4.2. Comparison to Standard 2D MUSIC Estimator. In this simulation, the performance of the proposed algorithm is compared with the results by utilizing standard 2D MUSIC estimator. The standard 2D MUSIC method is concerned with source localization under the assumption that the sources are uncorrelated. However, when the sources are highly correlated or coherent, the signal subspace and noise subspace of covariance matrix do not conform to the requirement of orthogonality, which will lead to severe degradation in the localization performance. In contrast, the proposed sparse representation technique employs singular value decomposition of covariance matrix and does not rely on the orthogonality of the signal and noise subspaces. The grid size and SNR of both methods are set as $(\Delta\phi = 1^\circ, \Delta\theta = 1^\circ)$ and 0 dB, respectively. Other simulation parameter settings are the same as in the previous subsection. Two equal power sources impinge on the UCA from 2D DOA $(\phi = 90^\circ, \theta = 35^\circ)$ and $(\phi = 90^\circ, \theta = 55^\circ)$. The spatial spectrum of the mentioned sources is shown in Figures 3 and 4, where the red lines in Figures 3(a), 3(b), 4(a), and 4(b) represent the real 2D DOA, the dotted blue curves and solid red curves in Figures 3(c) and 4(c), respectively, represent

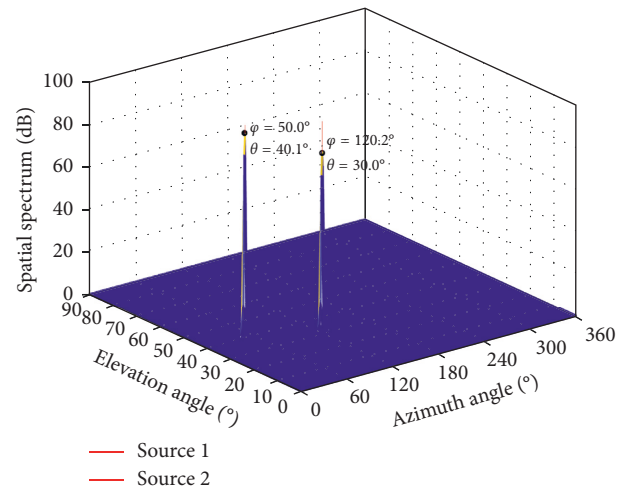

Figure 2: Spatial spectrum by employing the proposed SR method (SNR = 0 dB).

elevation angle spectrum when the azimuth angle ϕ is set at 90°.

When the two sources are incoherent and the frequencies are, respectively, set at 100 MHz and 101 MHz, it can be noticed from Figures 3(a)–3(c) that the proposed sparse representation technique and the standard 2D MUSIC method are able to resolve the two incoherent sources and obtain 2D DOA estimation. The sidelobes of proposed sparse representation technique in Figure 3(c) are suppressed almost to −100 dB, which can conclude that the proposed algorithm achieve more superresolution localization of incoherent sources than the standard 2D MUSIC method.

Next, we consider the sources are coherent and the frequencies are both set at 100 MHz. It can be noticed from Figures 4(a)–4(c) that the proposed sparse representation technique can decouple the coherent sources and obtain two sharp peaks in spatial spectrum which are corresponding to the 2D DOA estimation, whereas the standard 2D MUSIC method merges the two peaks and has only one peak in spatial spectrum. We can conclude that the proposed sparse representation technique can handle coherent sources localization while the standard 2D MUSIC cannot.

4.3. Sensitivity to the Assumed Number of Sources. In this simulation, the performance of the proposed algorithm under different assumed source number is considered. The coherent sources impinge on the UCA from 2D DOA $(\phi = 90^\circ, \theta = 10^\circ)$ and $(\phi = 90^\circ, \theta = 60^\circ)$ when SNR is set as 10 dB. The frequencies of the two coherent sources are both set at 100 MHz. The grid size of elevation angle is set as $\Delta\theta = 0.1^\circ$ and the azimuth angle is known to set as $\phi = 90^\circ$. The snapshot number N is set as 50, and the assumed number of sources G in (17) changes from 1 to 4.

The elevation angle spectrum of proposed SR method in different assumed number of coherent sources is shown in Figure 5. It can be noticed that the proposed approach is not sensitive to the assumed number of coherent sources and

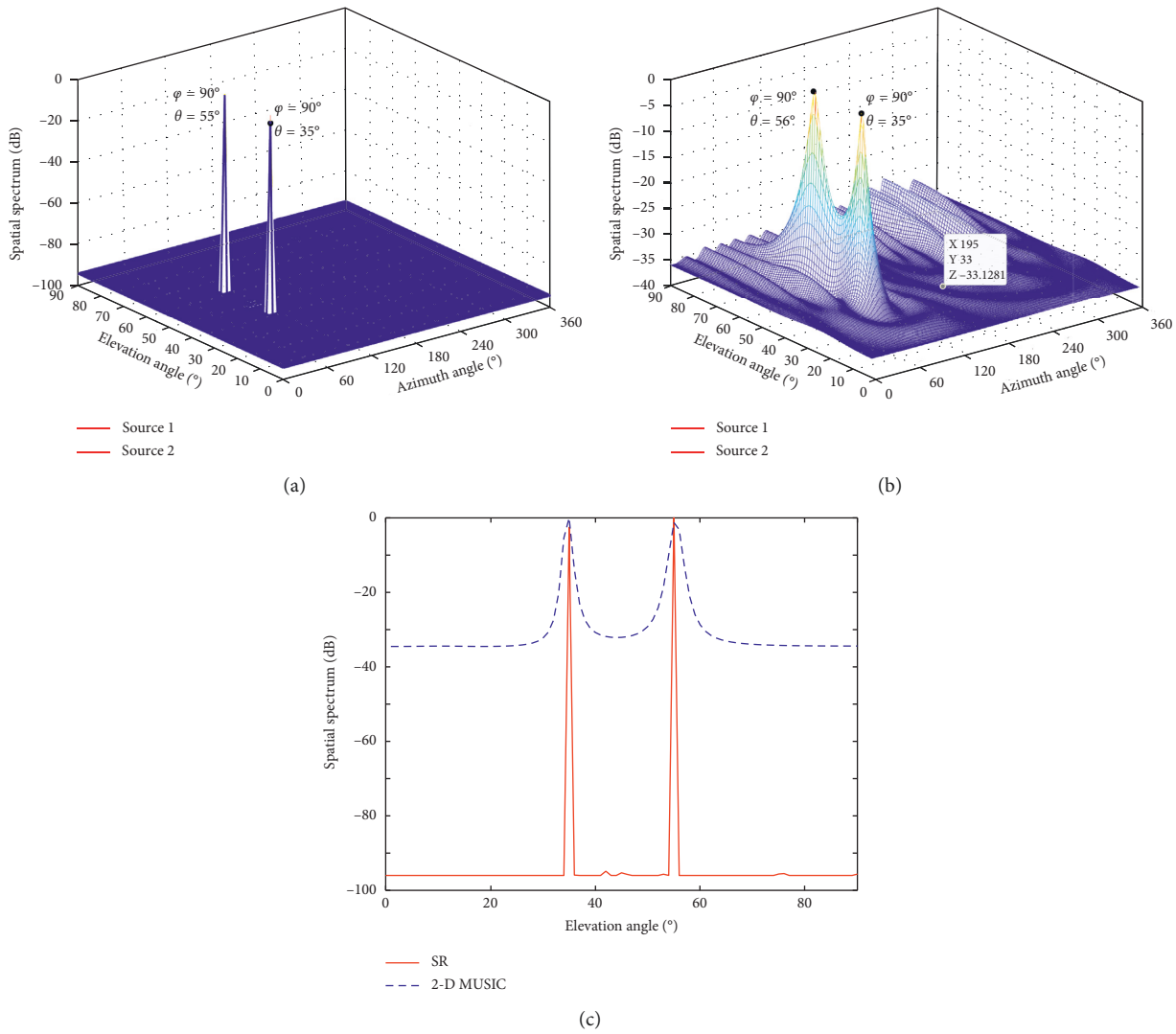

Figure 3: The comparison of incoherent source spectrum (SNR = 0 dB). (a) Spatial spectrum by SR method. (b) Spatial spectrum by standard 2D MUSIC method. (c) Elevation angle spectrum ($\varphi = 90^\circ$).

does not need to know real number in advance. Because the proposed approach does not depend on the orthogonality of the signal space and the noise space, the assumed number of coherent sources can only affect the computational complex. In addition, due to the convexity of all optimization processes involved in the approach, the number of inaccurate sources will not have disastrous effect for 2D DOA estimation when the number of sources is unknown.

4.4. RMSE and Resolution Probability of 2D DOA Estimation. In this simulation, the performance of the proposed algorithm is compared with the results by utilizing smoothed 2D MUSIC estimator. The grid size both methods are set as $(\Delta\phi = 1^\circ, \Delta\theta = 1^\circ)$. Other simulation parameter settings are the same as in the previous subsection. Based on the standard method, the smoothed 2D MUSIC method in [10] employs a preprocessing technique that extends the application of spatial smoothing to achieve coherent source localization, which transforms uniform circular array to a virtual array and restores the rank of covariance matrix to the number of coherent sources.

The root mean square error (RMSE) at each SNR is calculated by the average of 500 independent Monte Carlo simulations for the mentioned coherent sources, which is defined as

$$\mathrm{RMSE}(\beta) = \sqrt{\frac{1}{N_{\mathrm{MC}}K}\sum_{n_{\mathrm{MC}}=1}^{N_{\mathrm{MC}}}\sum_{k=1}^{K}\left(\widehat{\beta}_{\mathrm{mc}} - \beta_{\mathrm{mc}}\right)^2}, \tag{22}$$

where N_{MC} and K denotes the number of Monte Carlo simulations and the number of coherent sources, $\widehat{\beta}$ represents the 2D DOA estimation (azimuth angle $\widehat{\phi}$ or elevation angle $\widehat{\theta}$), and β represents the real 2D DOA of coherent sources.

When the snapshot number is set as 1000, the RMSEs of the azimuth angle and elevation angle at different SNR are given in Figures 6(a)–6(b), where the curves in red color represent the RMSEs of the proposed sparse representation

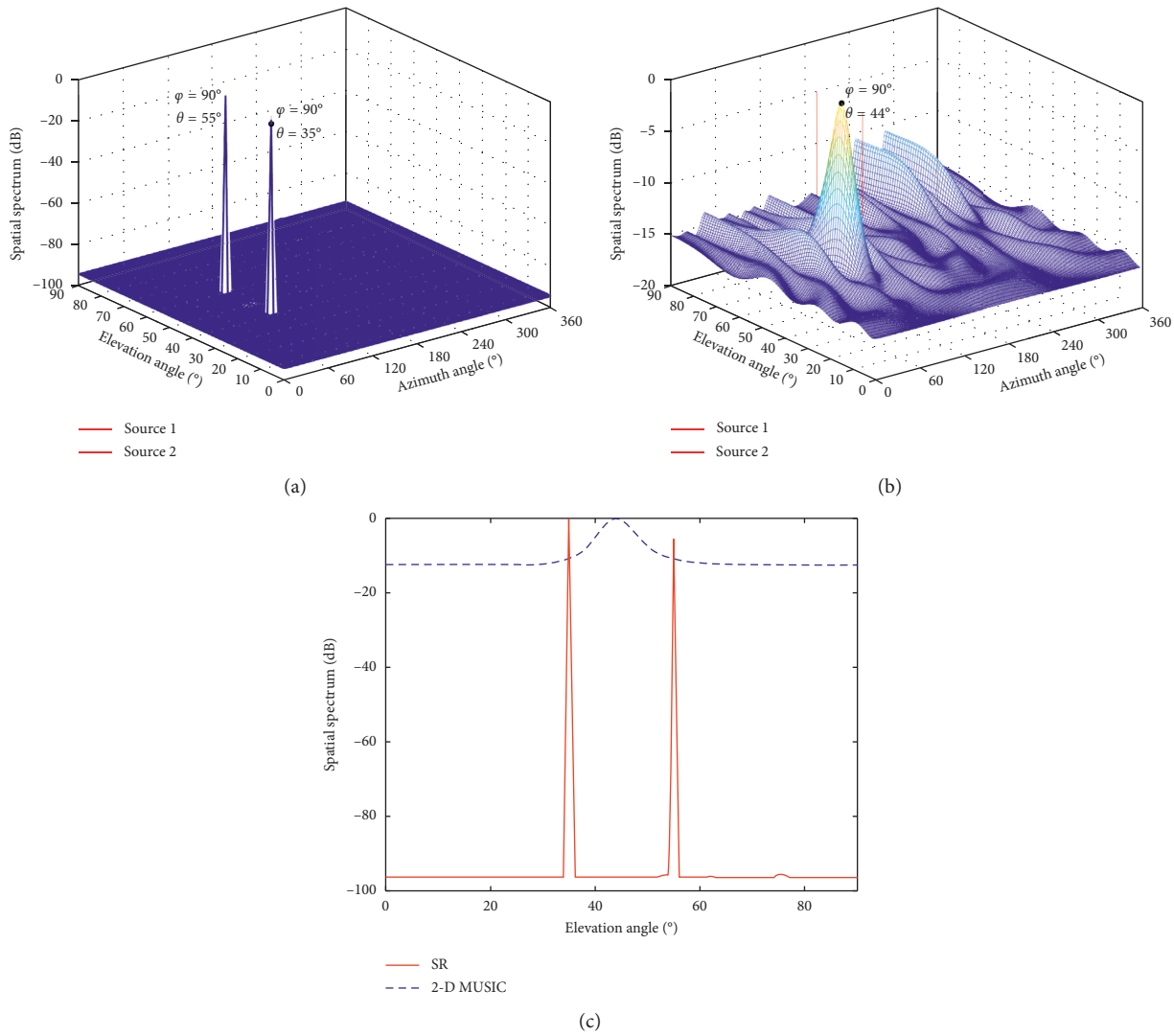

Figure 4: The comparison of coherent source spectrum (SNR = 0 dB). (a) Spatial spectrum by SR method. (b) Spatial spectrum by standard 2D MUSIC method. (c) Elevation angle spectrum ($\varphi = 90^\circ$).

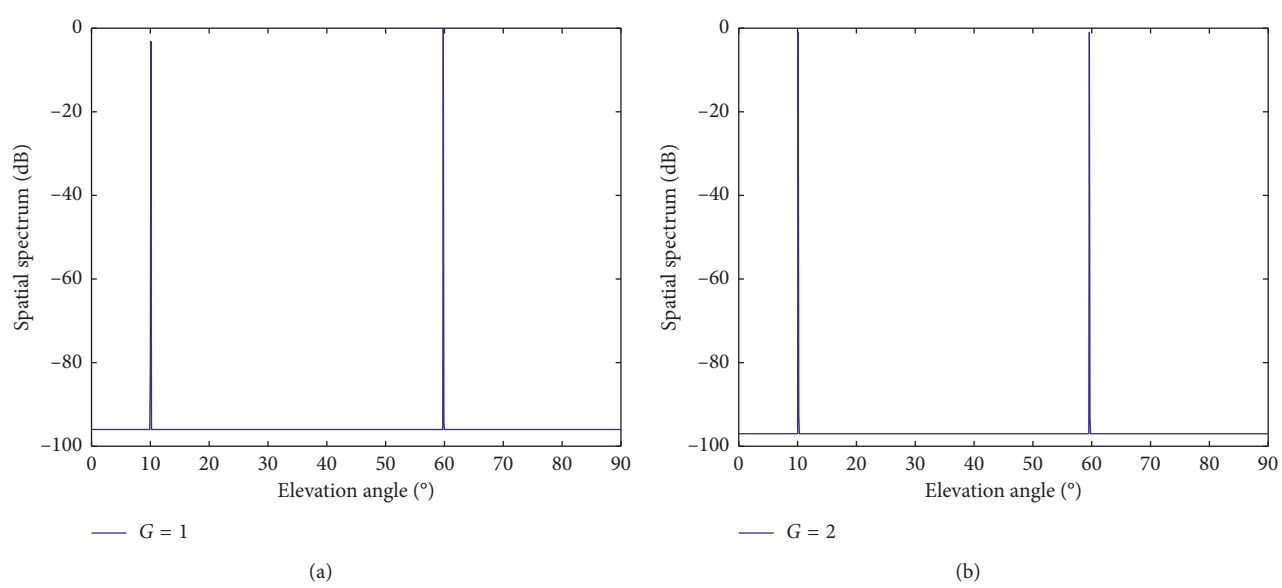

Figure 5: Continued.

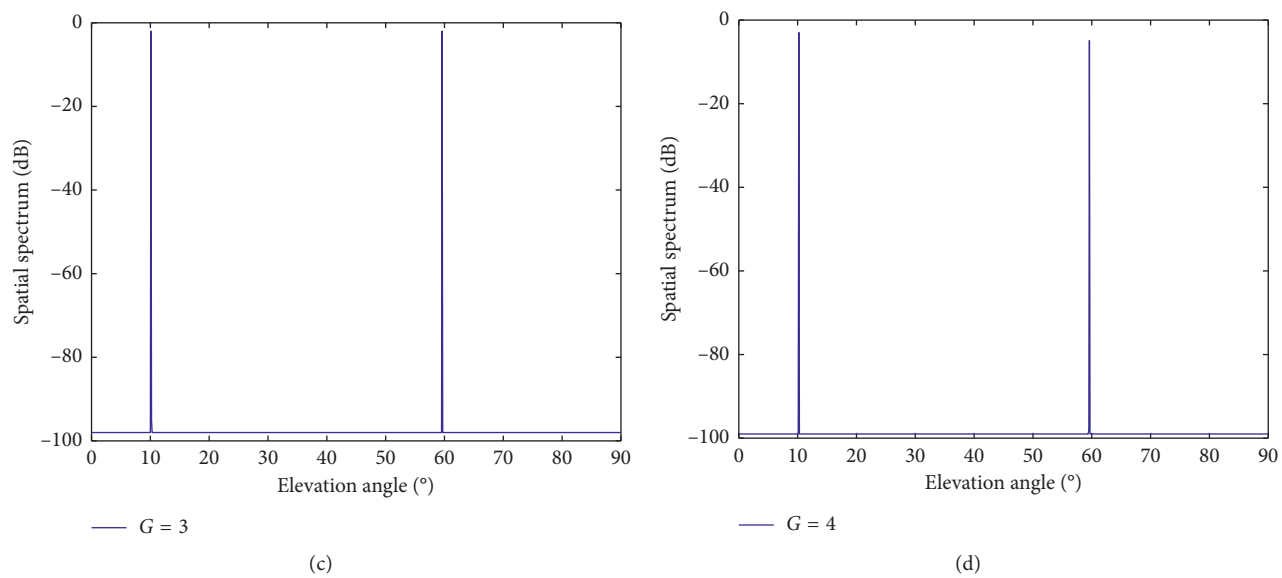

Figure 5: The elevation angle spectrum of proposed SR method under different assumed number of coherent sources (SNR = 10 dB). (a) $G = 1$. (b) $G = 2$. (c) $G = 3$. (d) $G = 4$.

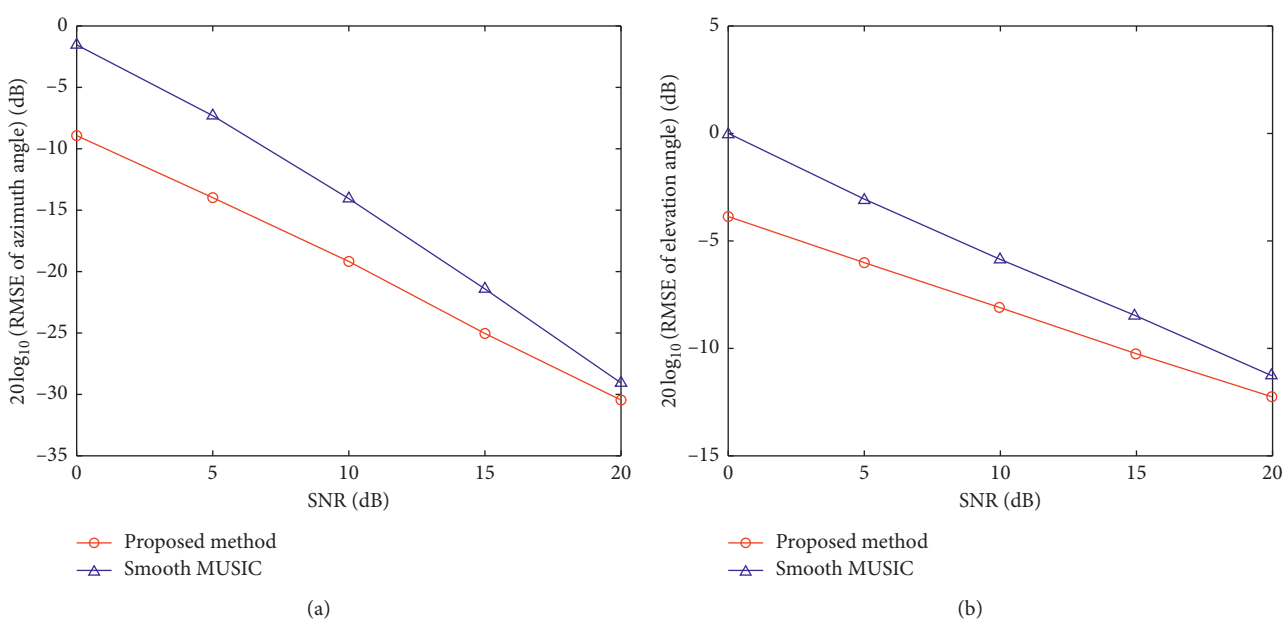

Figure 6: RMSEs versus SNR. (a) Azimuth angle. (b) Elevation angle.

method, the curves in blue color represent that of smoothed 2D MUSIC method, respectively. It can be noticed that the proposed sparse representation algorithm and smoothed 2D MUSIC method can achieve coherent source localization with increased SNR. Besides, the results show that the proposed sparse representation algorithm can achieve more superresolution localization of coherent sources than the smoothed 2D MUSIC method especially in the case of low SNR.

With regards to the resolution probability, we verify the resolution ability of the proposed sparse representation algorithm and the smoothed 2D MUSIC method by calculating the ratio between the number of successful estimations and the number of total simulations. The 2D DOA of two closely placed coherent sources are set as $(\phi = 60^\circ, \theta = 30^\circ)$ and $(\phi = 63^\circ, \theta = 33^\circ)$, respectively. The resolution probability at each SNR or snapshot number is calculated by 500 independent Monte Carlo simulations for the mentioned coherent sources.

When the snapshot number is set as 1000, the resolution probabilities versus SNR are shown in Figure 7(a). Similarly, when the SNR is set as 10 dB, the resolution probabilities

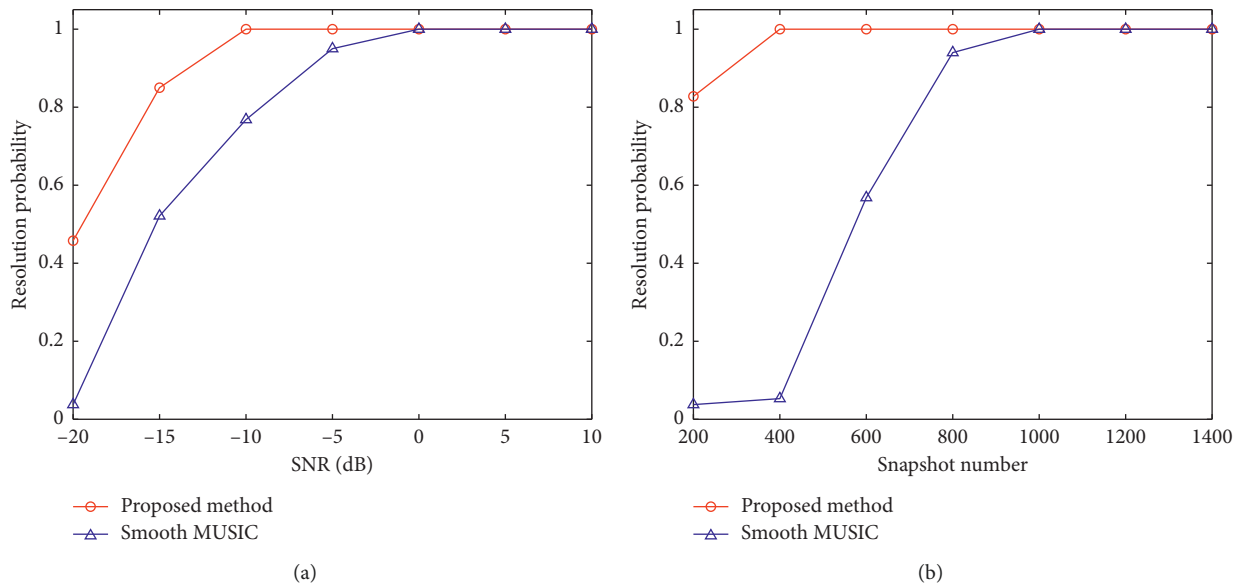

Figure 7: Resolution probabilities versus different parameters. (a) SNR. (b) Snapshot number.

versus snapshot number are shown in Figure 7(b), where the curves in red color represent the resolution probabilities of the proposed sparse representation method, and the curves in blue color represent that of smoothed 2D MUSIC method, respectively. It can be noticed that the resolution ability of the both methods is improved as the value of SNR or snapshot number increases. Besides, we can conclude that the proposed sparse representation algorithm has better resolution ability than the smoothed 2D MUSIC method especially in the case of low SNR or limited snapshot number.

5. Conclusions

This paper has presented a sparse representation method to obtain superresolution 2D DOA for coherent sources with a uniform circular array. We compute the ℓ_2 norm of time samples in spatial index and utilize SVD of the data matrix to reduce computational complexity. Besides, we employ SOC programming to solve convex optimization problem and obtain 2D superresolution spatial spectrum. The advantage of our proposed method for coherent source localization is that the resolution ability is better than the smoothed 2D MUSIC method especially in the case of low SNR or limited snapshot number. Moreover, the results show that the proposed SR approach does not need to estimate the number of sources in advance, and the localization performance is not sensitive to assumed number of coherent sources.

Data Availability

The data used to support the findings of this study are available from the corresponding author upon request.

Conflicts of Interest

The authors declare no conflicts of interest.

Authors' Contributions

The main IDEA was proposed by Xiaolong Su and Zhen Liu; Xiaolong Su and Tianpeng Liu conceived and designed the experiments; Xiaolong Su and Bo Peng wrote the paper; and Xin Chen and Xiang Li revised the paper.

Acknowledgments

This work is supported in part by the National Natural Science Foundation of China (no. 61401481) and in part by the Natural Science Foundation of Hunan Province, China (no. 2017JJ3368).

References

[1] P. R. Singh, Y. Wang, and P. Chargé, "Bistatic MIMO radar for near field source localisation using PARAFAC," *Electronics Letters*, vol. 52, no. 12, pp. 1060-1061, 2016.

[2] H. Yu, X. Zhang, X. Chen, and H. Wu, "Computationally efficient DOA tracking Algorithm in monostatic MIMO radar with automatic association," *International Journal of Antennas and Propagation*, vol. 2014, Article ID 501478, 10 pages, 2014.

[3] N. Wu, Z. Qu, W. Si, and S. Jiao, "DOA and polarization estimation using an electromagnetic vector sensor uniform circular array based on the ESPRIT algorithm," *Sensors*, vol. 16, no. 12, p. 2109, 2016.

[4] L. Li, F. Chen, and J. Dai, "Separate DOD and DOA estimation for bistatic MIMO radar," *International Journal of Antennas and Propagation*, vol. 2016, Article ID 9170403, 11 pages, 2016.

[5] R. Goossens, H. Rogier, and S. Werbrouck, "UCA Root-MUSIC with sparse uniform circular arrays," *IEEE Transactions on Signal Processing*, vol. 56, no. 8, pp. 4095–4099, 2008.

[6] B. R. Jackson, S. Rajan, B. J. Liao, and S. Wang, "Direction of arrival estimation using directive antennas in uniform circular arrays," *IEEE Transactions on Antennas and Propagation*, vol. 63, no. 2, pp. 736–747, 2015.

[7] X. Chen, Z. Liu, and X. Wei, "Unambiguous parameter estimation of multiple near-field sources via rotating uniform circular array," *IEEE Antennas and Wireless Propagation Letters*, vol. 16, pp. 872–875, 2017.

[8] Z. Liu, X. Chen, Z. Wei et al., "Ambiguity analysis and resolution for phase-based 3-D source Localization under given UCA," *International Journal of Antennas and Propagation*, vol. 2019, Article ID 4743829, 12 pages, 2019.

[9] X. Su, Z. Liu, X. Chen, and X. Wei, "Closed-form algorithm for 3-D near-field OFDM source localization under uniform circular array," *Sensors*, vol. 18, no. 5, p. 1432, 2018.

[10] M. Wax and J. Sheinvald, "Direction finding of coherent signals via spatial smoothing for uniform circular arrays," *IEEE Transactions on Antennas and Propagation*, vol. 42, no. 5, pp. 613–620, 1994.

[11] T. J. Shan, M. Wax, and T. Kailath, "On spatial smoothing for direction-of- arrival estimation coherent signal," *IEEE Transactions on Acoustics, Speech, and Signal Processing*, vol. 33, no. 4, pp. 806–811, 1985.

[12] A. H. Tewfik and W. Hong, "On the application of uniform linear array bearing estimation techniques to uniform circular arrays," *IEEE Transactions on Signal Processing*, vol. 40, no. 4, pp. 1008–1011, 1992.

[13] D. Malioutov, M. Cetin, and A. S. Willsky, "A sparse signal reconstruction perspective for source localization with sensor arrays," *IEEE Transactions on Signal Processing*, vol. 53, no. 8, pp. 3010–3022, 2005.

[14] C. P. Mathews and M. D. Zoltowski, "Eigenstructure techniques for 2-D angle estimation with uniform circular arrays," *IEEE Transactions on Signal Processing*, vol. 42, no. 9, pp. 2395–2407, 1994.

[15] E. J. Candes and M. B. Wakin, "An introduction to compressive sampling," *IEEE Signal Processing Magazine*, vol. 25, no. 2, pp. 21–30, 2008.

[16] P. Stoica, P. Babu, and J. Li, "SPICE: SPICE: a sparse covariance-based estimation method for array processing," *IEEE Transactions on Signal Processing*, vol. 59, no. 2, pp. 629–638, 2011.

[17] Z. Q. He, L. N. Jin, Q. H. Liu, and S. Ouyang, "Low complexity method for DOA estimation using array covariance matrix sparse representation," *Electronics Letters*, vol. 49, no. 3, pp. 228–230, 2013.

[18] S. Chang, Y. Li, H. Wang, W. Hu, and Y. Wu, "RSS-based cooperative localization in wireless sensor networks via second-order cone relaxation," *IEEE Access*, vol. 6, pp. 54097–54105, 2018.

[19] E. Fishler, M. Grosmann, and H. Messer, "Detection of signals by information theoretic criteria: general asymptotic performance analysis," *IEEE Transactions on Signal Processing*, vol. 50, no. 5, pp. 1027–1036, 2002.